

## VI. APPLIED PLASMA RESEARCH

### A. Active Plasma Systems

#### Academic Research Staff

Prof. L. D. Smullin  
Prof. A. Bers

Prof. R. R. Parker  
Prof. K. I. Thomassen

#### Graduate Students

N. J. Fisch  
S. P. Hirshman  
C. F. F. Karney  
J. L. Kulp

G. H. Neilson  
J. J. Schuss  
M. D. Simonutti

M. S. Tekula  
A. L. Throop  
D. C. Watson  
P. R. Widing

### 1. EFFICIENCY CONSIDERATIONS FOR A PLASMA GUN SYSTEM

National Science Foundation (Grant GK-28282X1)

S. P. Hirshman, L. D. Smullin

As reported in Quarterly Progress Report No. 105 (pp. 89-93), we have been studying the efficiency of electrical energy conversion to plasma energy in a plasma gun system. This report gives a summary of our latest results.<sup>1</sup>

#### General Efficiency Criteria

Several measures of efficiency have been proposed by Jahn<sup>2</sup> and Mendel.<sup>3</sup> The dynamic efficiency is defined by

$$\eta_d = \frac{\frac{1}{2} m v_s^2}{W_p},$$

where  $W_p = \int_0^t \mathbf{f}^m \cdot \mathbf{v}_s \, d\tau$  is the total work done on the sheet gas by the magnetic forces (including shock heating). In this measure of efficiency, only the final mass motion of the plasma is considered as a figure of merit. An alternative definition is the electro-mechanical efficiency, a measure of the ability to couple electric energy into total plasma energy,

$$\eta_{em} = \frac{W_p}{E_o},$$

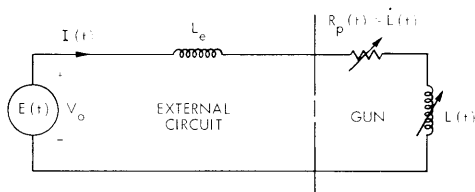
where  $E_o$  is the initial energy stored in the external power supply. This efficiency takes into account the fact that gas particles undergoing inelastic collisions with the snowplow piston are heated and thus represent a useful conversion of electric energy into plasma

(VI. APPLIED PLASMA RESEARCH)

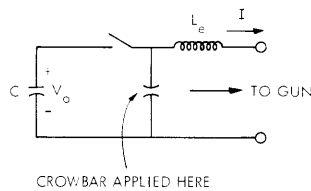
energy. Finally, the kinetic efficiency, a measure of the ability to couple electrical energy to energy of motion of the sheet, is defined by

$$\eta_K = \frac{\frac{1}{2} m v_s^2}{E_o}$$

Note that  $\eta_K = \eta_d \eta_{em}$ ; therefore,  $\eta_K$  is always less than either  $\eta_d$  or  $\eta_{em}$ . The choice of  $\eta$  to be used in any efficiency analysis depends on the particular task for which the gun is to be used. For ion thrusters,  $\eta_K$  is the relevant efficiency to optimize, while for plasma injection applications, both  $\eta_K$  and  $\eta_{em}$  are useful efficiency measures.



(a)



(b)

Fig. VI-1.

(a) General gun circuit. (b) Capacitor bank with crowbar.

To obtain physical insight into the dependence of  $\eta_K$  and  $\eta_{em}$  on circuit and gun parameters, it is useful to express all variables in terms of the external circuit energy  $E(t)$  (Fig. VI-1a) and the gun inductance  $L(t)$ , which is proportional to the instantaneous sheet position and hence representative of the "state" of the sheet in the accelerator. The result<sup>1</sup> is

$$\eta_{em} = \frac{1 - \frac{\int_0^{L_f} E dL}{E_o L_f}}{1 + \frac{C}{L_f}}, \quad (1)$$

and

$$\eta_K = \eta_{em} - \frac{1}{2 \sqrt{m_f}} \int_0^{t_f} \frac{\dot{m}}{\sqrt{m}} \eta_{em}(\tau) d\tau, \quad (2)$$

where subscript f refers to the final accelerator state. It is clear that to optimize  $\eta_{em}$ ,  $L_f \gg L_e$  is desirable; furthermore, the externally stored energy should be supplied to the gun as quickly as possible and remain out of the external circuit. One way to prevent energy E from returning to the power circuit is to crowbar the power supply when E is at minimum. A typical circuit of this kind, which will be analyzed in greater detail, is shown in Fig. VI-1b.

The second term in Eq. 2 represents losses from shock heating, and the effect on efficiency is not as readily interpreted as  $\eta_{em}$  was before.

### Independent Parameters of a Gun System

In any real gun system, there are numerous performance requirements that impose constraints on the otherwise independent gun parameters. For injection (or thruster) applications, the type of working gas, the final velocity, and the kinetic energy of the accelerated plasma are to be considered prescribed by the requirements imposed by heating capabilities, plasma penetration into magnetic fields, and so forth. These three constraints are sufficient to allow an optimum determination of all other system parameters. (In a practical system, the inductance per unit length  $\mathcal{L}$  is severely restricted by geometrical considerations and should be chosen as large as possible; cf. Eq. 1.)

Our procedure consists in solving a normalized set of equations<sup>1</sup> which completely describes the gun system of Fig. VI-1b. For a uniform distribution of filling gas, we found that  $\eta_K$  and  $\eta_{em}$  depend only on two coupling parameters:

(i) Energy parameter,  $\epsilon \equiv E_o / L_o I_o^2$ . Physically,  $\epsilon$  is a measure of the energy "match" between the gun and the external circuit.

(ii) Time parameter,  $\mu = t_o / t_c$ , where  $t_o = l / u_o$ , with  $u_o$  the snowplow velocity, and  $t_c = E_o / V_o I_o$ . Here  $\mu$  is a measure of the matching of circuit ( $t_c$ ) and intrinsic ( $t_o$ ) gun time scales.

In the particular case considered here,  $E_o = \frac{1}{2} CV_o^2$  and  $I_o^2 = CV_o^2 / L_o$ , so that  $\epsilon = \frac{1}{2} \frac{L_e}{L_o}$ , and  $\mu = 2t_o / (LC)^{1/2}$ .

Therefore, for any gun system driven by a capacitor bank and obeying the snowplow dynamics, the efficiency of energy conversion depends only on the two parameters  $\epsilon$  and  $\mu$ . Furthermore, with  $M_o$ ,  $m_i$ , and  $u_f = \frac{\kappa(\epsilon, \mu)}{\sqrt{2}} u_o$  specified, the remaining system parameters can be expressed solely in terms of  $\epsilon$  and  $\mu$ , provided we make an optimum choice of system length.<sup>1</sup>

There is an efficiency,  $\eta_j$ , associated with any pair of coordinates ( $\epsilon, \mu$ ). In general, there will be level curves of constant  $\eta_j$  in  $\epsilon, \mu$  space, and any point in this space for which  $\eta_j$  is a maximum represents an optimum solution to the efficiency problem. There are, however, certain practical constraints that limit the region of accessibility

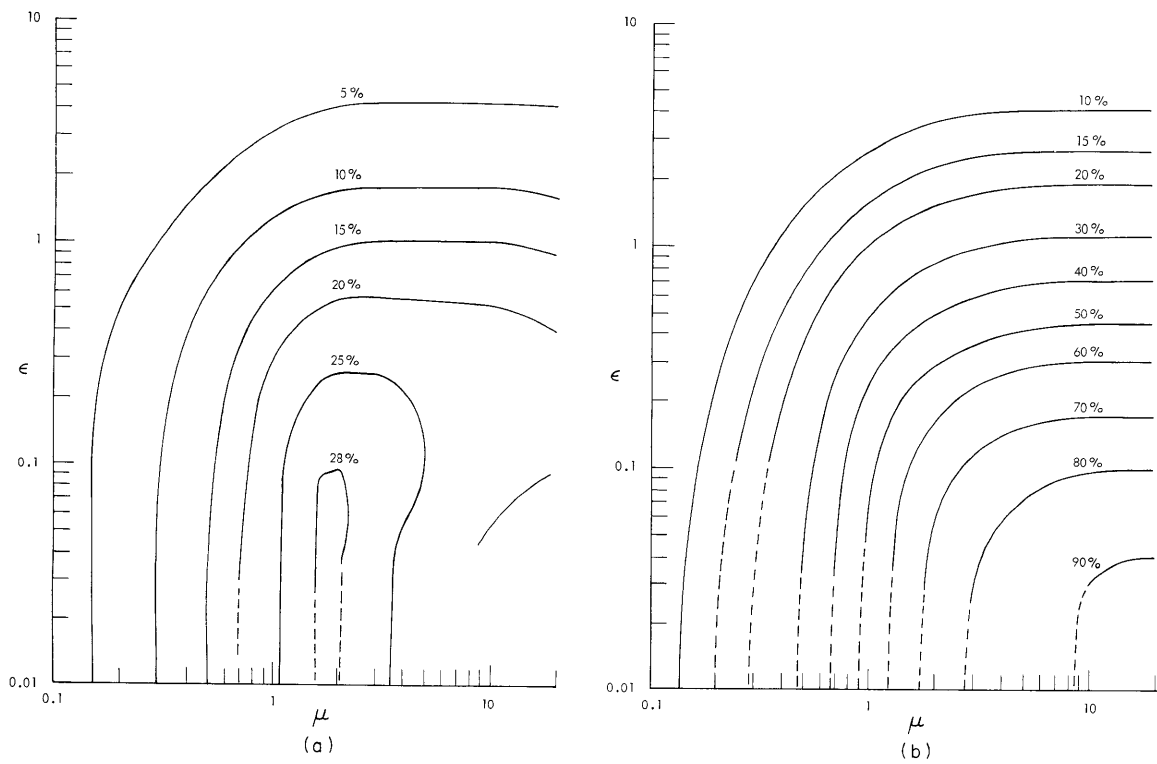


Fig. VI-2. (a) Kinetic efficiency level curves.  
 (b) Electromechanical efficiency level curves.

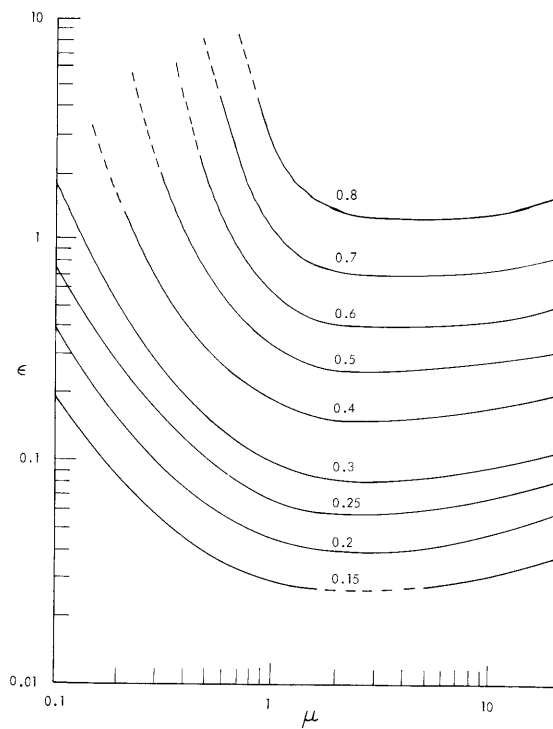


Fig. VI-3. Final velocity fraction ( $\kappa$ ) curves.

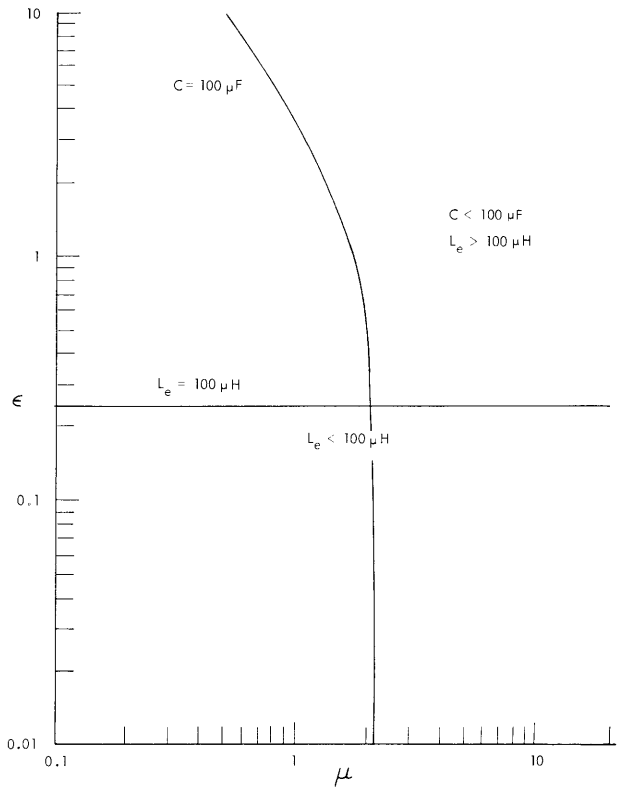
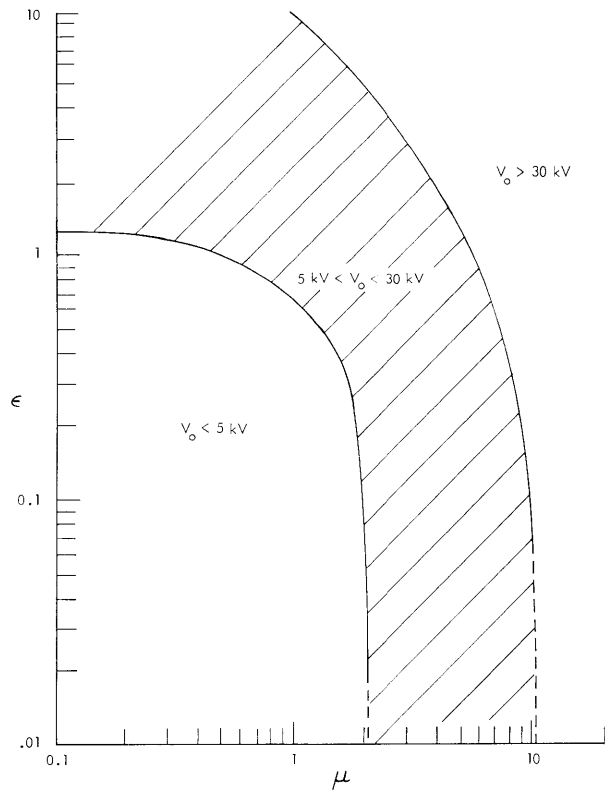


Fig. VI-4. Typical constraints  $V_o$ ,  $C$ ,  $L_e$ .

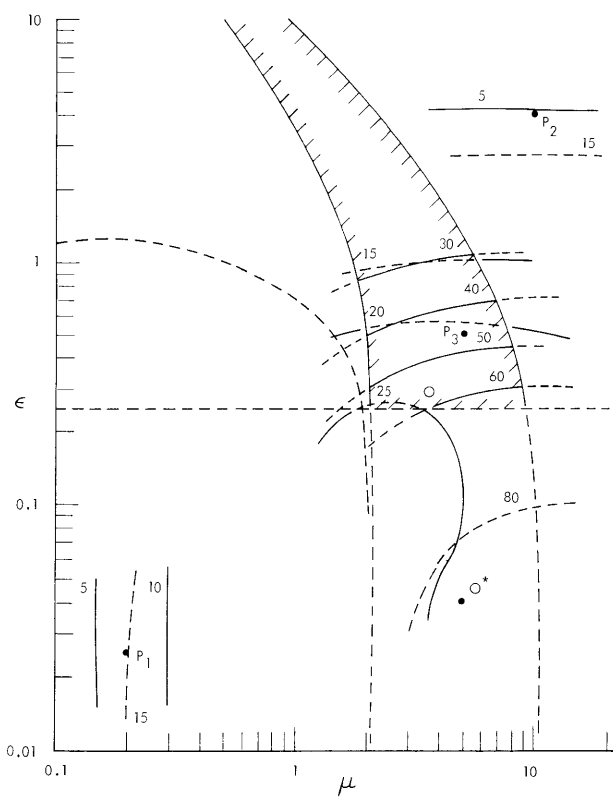


Fig. VI-5.

Intersections of regions of accessibility (net region shaded).  $O$  ( $\epsilon = 0.25$ ,  $\mu = 3.5$ ) is the point of optimum attainable efficiency.

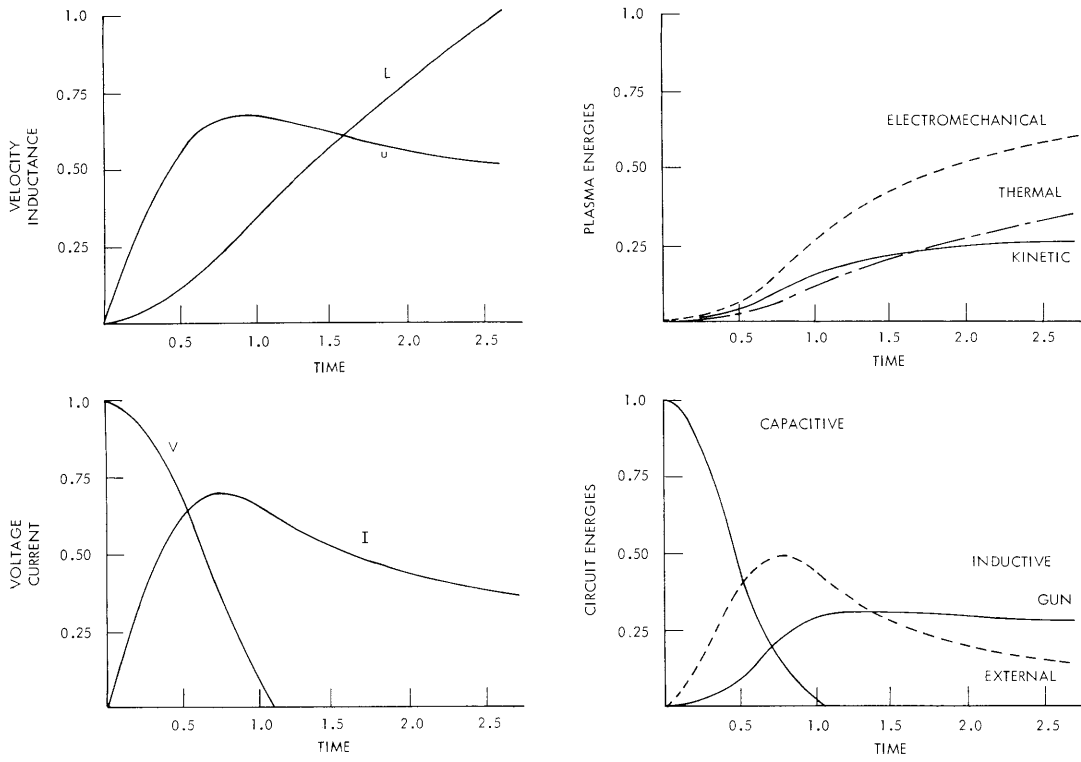


Fig. VI-6.  $\circ$  ( $\epsilon = 0.25$ ,  $\mu = 3.5$ ): Optimum realizable parameters.

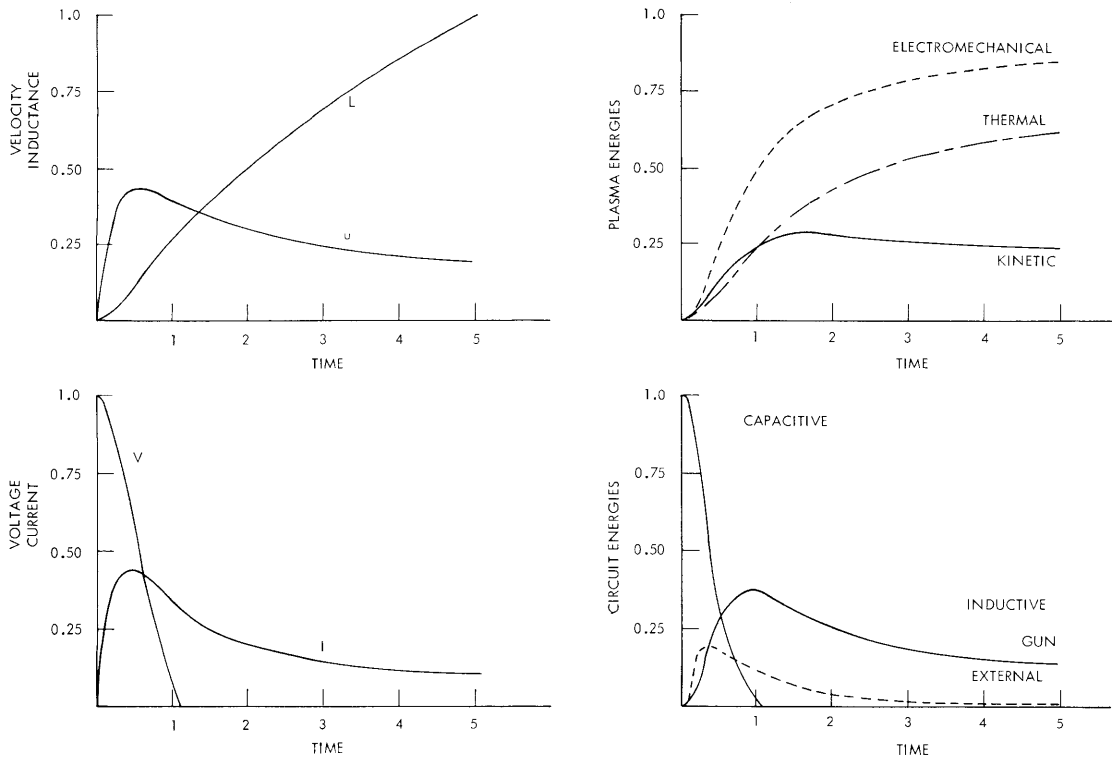


Fig. VI-7.  $\circ^*$  ( $\epsilon = 0.04$ ,  $\mu = 5$ ): Optimum parameters.

in  $\epsilon, \mu$  space, and hence the optimum value of  $\eta_j$ .

The contours of constant kinetic and electromechanical efficiencies were numerically computed and are shown in Fig. VI-2 for the  $\epsilon, \mu$  space of practical interest. Figure VI-3 shows curves of constant final velocity fraction  $\kappa(\epsilon, \mu)$ . Note the great sensitivity of the efficiency curves on  $\epsilon \sim L_e/L_0$ , as expected from Eq. 1.

Once these curves have been obtained, they can be used to design a plasma gun that will operate in the most efficient manner. The typical constraints  $5 \text{ kV} < V_0 < 30 \text{ kV}$ ,  $L_e \geq 10^{-7} \text{ H}$ , and  $C \leq 100 \text{ } \mu\text{F}$  are shown in Fig. VI-4 for hydrogen gas of total filling mass  $10^{-7} \text{ kg}$  and final velocity  $10^5 \text{ m/s}$ . In Figure VI-5, the intersection of all three constraints is plotted, with the net region of accessibility shaded. The point O ( $\epsilon = 0.25$ ,  $\mu = 3.5$ ) appears to be the point of optimum attainable efficiency for this design, and corresponds to  $\eta_K = 25\%$  and  $\eta_{em} = 60\%$ . The (normalized) system variables (velocity, current, voltage, efficiencies) are plotted in Fig. VI-6 for point O as functions of time. Note how the initial capacitive energy is entirely converted into inductive and plasma energy.

In Fig. VI-7 the point O\* ( $\epsilon = 0.04$ ,  $\mu = 5$ ) demonstrates the favorable effect obtained by lowering the circuit inductance  $L_e$  approximately an order of magnitude. Note the 25% gain in plasma efficiency over point O.

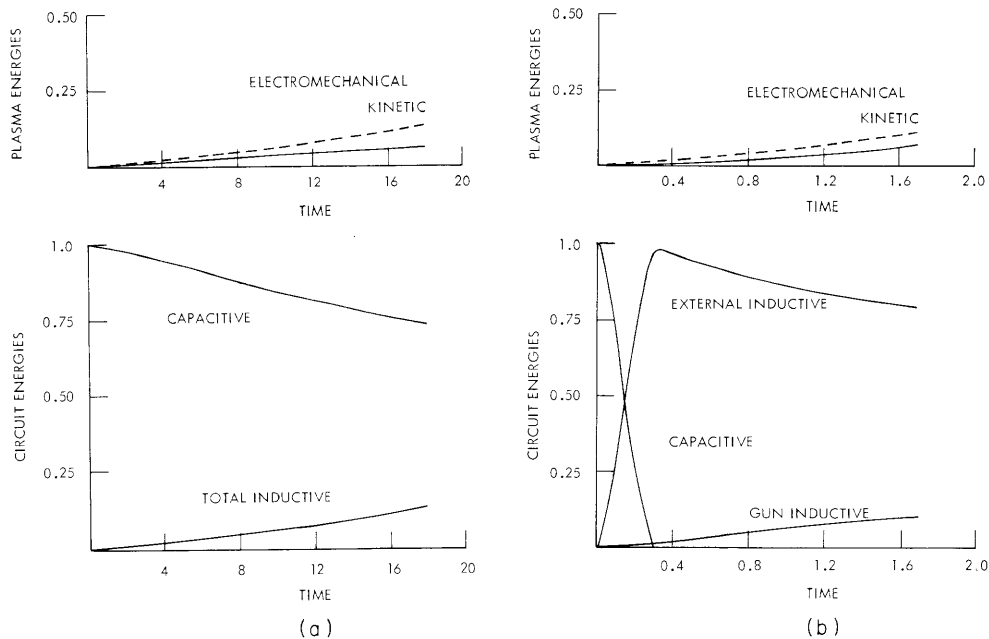


Fig. VI-8. Inefficient mode of operation.

(a)  $P_1$ :  $\epsilon = 0.025$ ,  $\mu = 0.2$ .

(b)  $P_2$ :  $\epsilon = 4$ ,  $\mu = 10$ .

## (VI. APPLIED PLASMA RESEARCH)

Furthermore, we may conclude that there are only two basically different ways in which the plasma gun system can operate inefficiently. These two cases are represented by  $P_1$  and  $P_2$  in Fig. VI-5, and correspond to small  $\mu$  and large  $\epsilon$  (and  $\mu$ ), respectively. When  $\mu$  is small, the gun is electrically "too short," and the acceleration process is over before the external circuit can transfer its energy to the plasma (Fig. VI-8a). When  $\epsilon$  (and  $\mu$ ) are large, energy is transferred only from the capacitor to the external inductor and never gets into the gun circuit. This inefficiency is illustrated in Fig. VI-8b.

### Conclusion

We have found that with reasonable circuit and gun parameters, it is possible to design a plasma gun that meets typical operating specifications with kinetic efficiency of 25% and overall plasma efficiency (including shock heating) of 60%. The efficiency estimates were based on a final plasma velocity of  $\sim 10^5$  m/s, which is (for hydrogen) below the thermonuclear threshold. It can be shown<sup>1</sup> that the effect of increasing the final velocity by a factor of 10 is to decrease the system efficiencies to  $\leq 5-10\%$ . Therefore, there is a severe reduction in system efficiency as the velocities required for thermonuclear applications are approached, a situation that casts doubt on the applicability of a plasma accelerator for thermonuclear heating.

### References

1. Detailed results are presented in S. P. Hirshman, S.M. Thesis, Department of Electrical Engineering, M.I.T., January 1973 (unpublished).
2. R. G. Jahn, Physics of Electric Propulsion (McGraw-Hill Book Company, Inc., New York, 1968).
3. C. W. Mendel, J. Appl. Phys. 42, 5483 (1971).



## VI. APPLIED PLASMA RESEARCH

### D. Laser-Plasma Interactions

#### Academic and Research Staff

Prof. E. V. George  
Prof. A. Bers

Prof. H. A. Haus  
Dr. P. A. Politzer  
Dr. A. H. M. Ross

J. J. McCarthy  
W. J. Mulligan

#### Graduate Students

Y. Manichaikul  
J. L. Miller

D. Prosnitz

C. W. Werner  
D. Wildman

### 1. SHORT PULSE PROPAGATION

National Science Foundation (Grant GK-33843)

A. H. M. Ross

A computer code has been developed to solve the wave equation for electromagnetic propagation in resonant media. While the ultimate goal of this effort is to produce a realistic numerical model of short-pulse amplifiers, including the effects of collisional exchange processes and rotational state degeneracy, preliminary testing with the idealized model of a two-level medium has produced new results concerning the so-called  $0\pi$  pulses.<sup>1</sup>

The one-dimensional wave equation in the slowly varying envelope approximation is

$$\frac{\partial \mathcal{E}}{\partial z} + \frac{1}{c} \frac{\partial \mathcal{E}}{\partial t} = -\frac{\sigma}{2y_0} \mathcal{E} - i \frac{\omega_0}{2y_0} \mathcal{P},$$

where  $\sigma$  is a phenomenological conductivity included to account for nonresonant losses,  $y_0 = \sqrt{\epsilon_0/\mu_0}$  is the admittance of free space, and  $\mathcal{E}$  and  $\mathcal{P}$  are the complex amplitudes of the electric field and polarization, respectively.

$$E(z, t) = \text{Re} [\mathcal{E}(z, t) \exp \{i(\omega_0 t - k_0 z)\}]. \quad (1)$$

Schrödinger's equation for a gaseous medium is most easily written in terms<sup>2</sup> of a density matrix distribution function  $\rho(z, v, t)$ .

$$\frac{d\rho}{dt} = -\frac{i}{\hbar} [H_0 - \vec{\mu} \cdot \vec{E}, \rho] + \left( \frac{d\rho}{dt} \right)_{\text{collision}},$$

where  $\frac{d}{dt} = \frac{\partial}{\partial t} + v \frac{\partial}{\partial z}$  is the convective derivative. The constitutive relation is

## (VI. APPLIED PLASMA RESEARCH)

$$P = n_0 \int_{-\infty}^{+\infty} dv \operatorname{Tr} (\mu \rho(z, v, t)),$$

where  $n_0$  is the mean particle density. The normalization of  $\rho$  is taken to be

$$\int_{-\infty}^{+\infty} dv \operatorname{Tr} (\rho) = 1.$$

For a system of two nondegenerate levels these relations become

$$\frac{\partial \rho_{aa}}{\partial t} = -\frac{\mu}{\hbar} \operatorname{Im} \left( \mathcal{E}^* \tilde{\rho}_{ab} \right) - \gamma_a \rho_{aa} + R_a \quad (2)$$

$$\frac{\partial \rho_{bb}}{\partial t} = +\frac{\mu}{\hbar} \operatorname{Im} \left( \mathcal{E}^* \tilde{\rho}_{ab} \right) - \gamma_b \rho_{bb} + R_b \quad (3)$$

$$\frac{\partial \tilde{\rho}_{ab}}{\partial t} = (ivk_{ab} - \gamma_{ab}) \tilde{\rho}_{ab} + i \frac{\mu}{2\hbar} \mathcal{E} (\rho_{aa} - \rho_{bb}) \quad (4)$$

$$\mathcal{P}(z, t) = 2n_0 \mu \int_{-\infty}^{+\infty} dv \tilde{\rho}_{ab}(z, v, t). \quad (5)$$

The collision term has been represented by phenomenological relaxation rates and pumping terms.

In the limit of very short pulse lengths, where all terms in (2)-(5) other than the electromagnetic ones can be neglected, analytical solutions of (1)-(5) can be found.<sup>1</sup> Among them are the  $n\pi$  pulses, which leave the medium in the same state after their passage as before their arrival. Particularly interesting are the pulses with bipolar envelopes such that their area is zero, the  $0\pi$  pulses. While most coherent propagation effects are drastically modified by degeneracy of the participating atomic levels, it has been shown, both theoretically<sup>1</sup> and experimentally,<sup>3</sup> that  $0\pi$  pulses can exist in more complicated media.

Since the closed-form solutions have been found only for completely unbroadened absorbing media, and because they cannot accommodate arbitrary inputs, it is necessary to use numerical methods for more realistic situations. Because of the interest in  $0\pi$  pulses, we present solutions of (1)-(5) in homogeneously and inhomogeneously broadened absorbing ( $\rho_{bb}(t=0) = 1$ ,  $\rho_{aa}(t=0) = 0$ ) gases for inputs that would otherwise be  $0\pi$  pulses.

As Lamb has shown,<sup>1</sup> there are two simple types of  $0\pi$  pulses. The first, illustrated in Fig. VI-9, separates into two relatively inverted  $2\pi$  pulses. The effect of finite phase damping is shown in Fig. VI-10 where the homogeneous linewidth has been

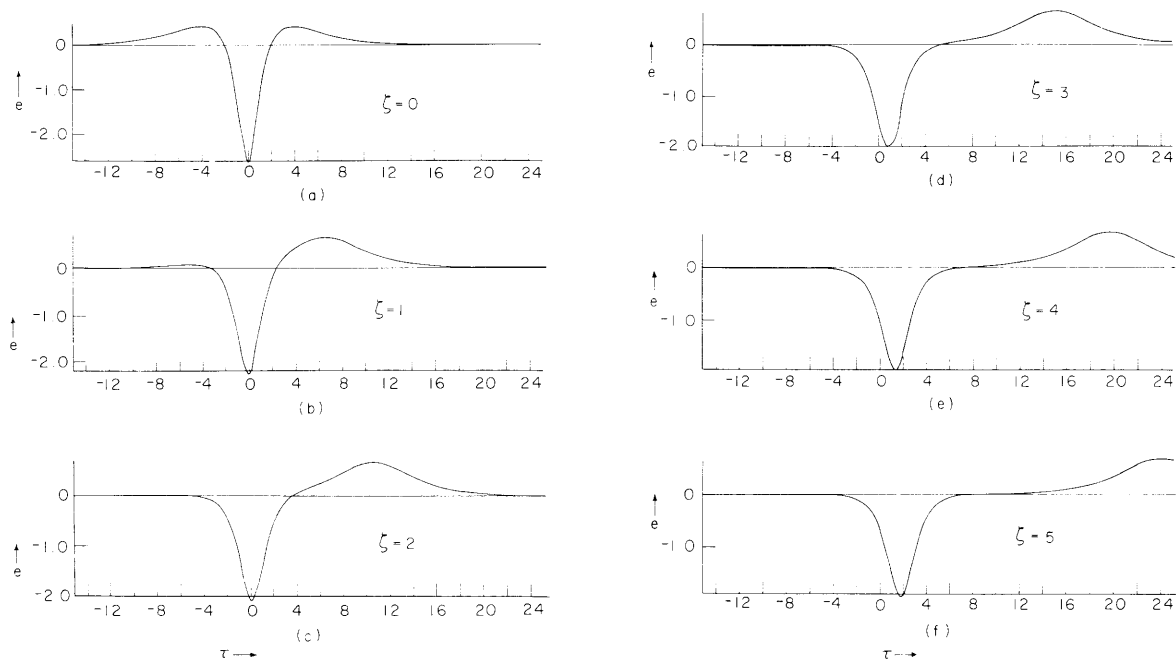


Fig. VI-9. Evolution of a separating  $0\pi$  pulse in a two-level medium of zero spectral width. Pulse widths:  $\tau_1 = 1$ ,  $\tau_2 = 3$ . Abscissa represents retarded time; ordinate the electric field envelope;  $\delta$  depth in medium. (All units dimensionless.)

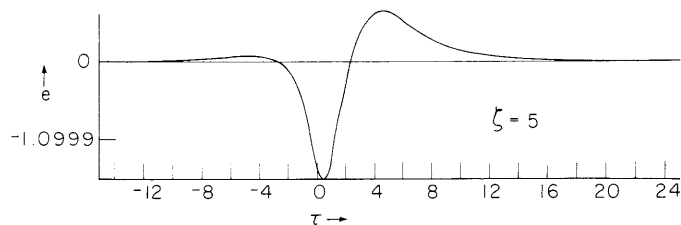


Fig. VI-10.

Separating  $0\pi$  pulse emerging from a homogeneously broadened attenuator:  $\gamma_{ab} = 1$ . (Other parameters as in Fig. VI-9.)

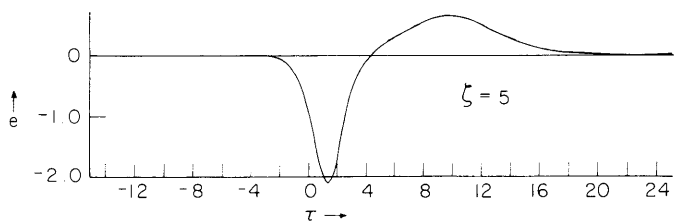


Fig. VI-11.

Separating  $0\pi$  pulse emerging from a Doppler-broadened attenuator:  $\Delta\omega_D = 1/\sqrt{2}$ . (Other parameters as in Fig. VI-9.)

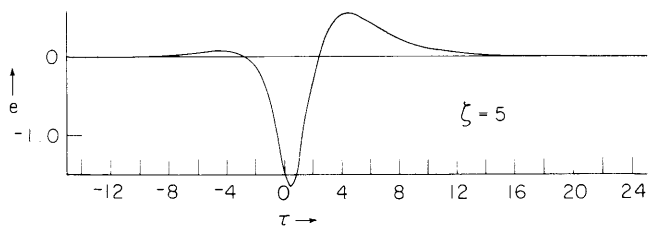


Fig. VI-12.

Separating  $0\pi$  pulse emerging from an attenuator with both broadening mechanisms:  $\gamma_{ab} = 1$ ,  $\Delta\omega_D = 1/\sqrt{2}$ . (Other parameters as in Fig. VI-9.)

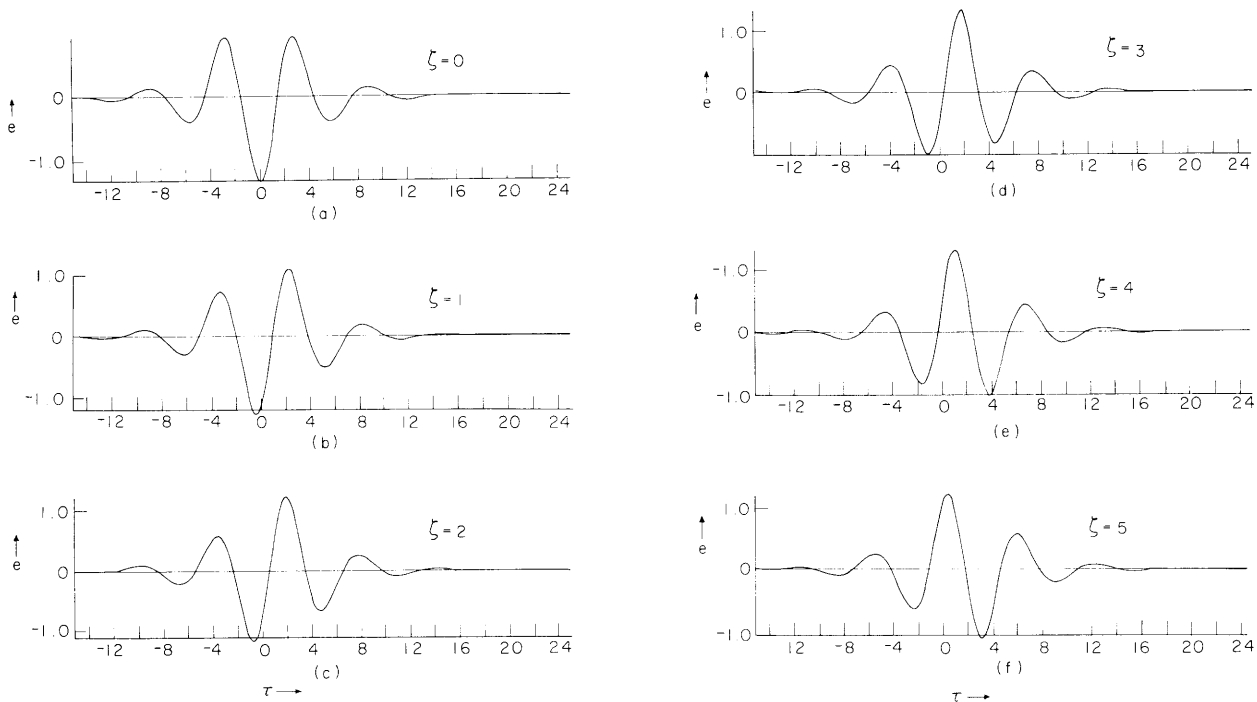


Fig. VI-13. Evolution of cohesive  $0\pi$  pulse in a two-level medium of zero spectral width. Pulse widths:  $\tau_1 = 1$ ,  $\tau_2 = 3$ .

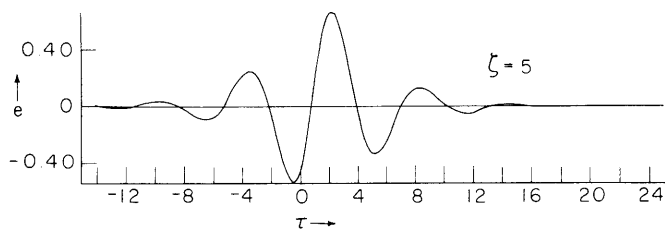


Fig. VI-14.

Cohesive  $0\pi$  pulse emerging from a homogeneously broadened attenuator:  $\gamma_{ab} = 1$ . (Other parameters as in Fig. VI-13.)

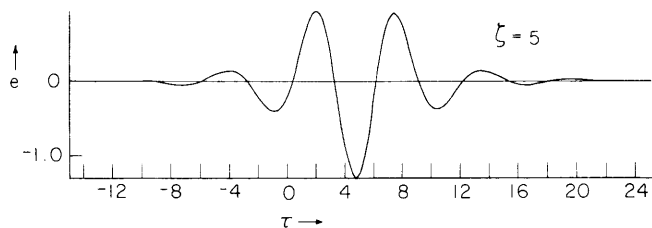


Fig. VI-15.

Cohesive  $0\pi$  pulse emerging from a Doppler-broadened attenuator:  $\Delta\omega_D = 1/\sqrt{2}$ . (Other parameters as in Fig. VI-13.)

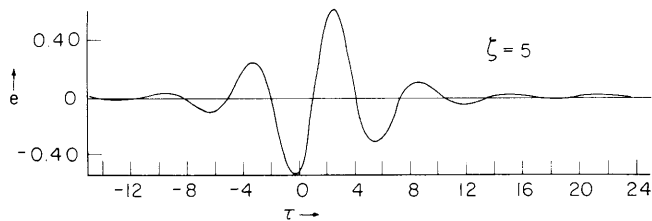


Fig. VI-16.

Cohesive  $0\pi$  pulse emerging from an attenuator with both broadening mechanisms:  $\gamma_{ab} = 1$ ,  $\Delta\omega_D = 1/\sqrt{2}$ . (Other parameters as in Fig. VI-13.)

chosen to be equal to the inverse pulse width of the shorter of the two pulses after separation. Figure VI-11 illustrates the same situation for inhomogeneous (Doppler) broadening with no phase damping. Figure VI-12 combines both broadening mechanisms.

The second type of  $0\pi$  pulse, in the absence of broadening, remains localized; it resembles a modulated hyperbolic secant in which the modulation varies with time. Figures VI-13 through VI-16 illustrate the effects of the various broadening mechanisms on this pulse. Note the relative insensitivity of this pulse to the pure inhomogeneous broadening. In all cases, however, energy loss to the medium eventually reduces the pulse to the linear regime.

Work continues on a more sophisticated model of a medium containing the effects of a rotation spectrum. This will be essentially a two-vibrational-level rotator that should provide a reasonably realistic model of many molecular lasers.

#### References

1. G. L. Lamb, Jr., "Analytical Descriptions of Ultrashort Optical Pulse Propagation in a Resonant Medium," *Rev. Mod. Phys.* 43, 99-124 (1971).
2. A. H. M. Ross, Ph.D. Thesis, Department of Electrical Engineering, M.I.T., June 1972.
3. H. P. Grieneisen, J. Goldhar, N. A. Kurnit, A. Javan, and H. R. Schlossberg, "Observation of the Transparency of a Resonant Medium to Zero-degree Optical Pulses," *Appl. Phys. Letters* 21, 559-562 (1972).

